proteomic analysis of cells exposed to prefibrillar aggregates of HypF-N

Biochimica et Biophysica Acta 1794 (2009) 1243–1250

Contents lists available at ScienceDirect

Biochimica et Biophysica Acta

journal homepage: www.elsevier.com/locate/bbapap

Proteomic analysis of cells exposed to prefibrillar aggregates of HypF-N

Francesca Magherini [a,*], Laura Pieri [a], Francesca Guidi [a], Chiara Giangrande [c], Angela Amoresano [c], Monica Bucciantini [a,b], Massimo Stefani [a,b], Alessandra Modesti [a]

[a] Dipartimento di Scienze Biochimiche, Università degli Studi di Firenze, Italy
[b] Research Centre on the Molecular Basis of Neurodegeneration, Università degli Studi di Firenze, Italy
[c] Dipartimento di Chimica Organica e Biochimica, Università di Napoli Federico II, Italy

ARTICLE INFO

Article history:
Received 16 February 2009
Received in revised form 20 April 2009
Accepted 21 April 2009
Available online 3 May 2009

Keywords:
2D-GE
MALDI-TOF
Prefibrillar protein aggregate
Protein expression profiling
HypF-N

ABSTRACT

Several human diseases are associated with the deposition of stable ordered protein aggregates known as amyloid fibrils. In addition, a large wealth of data shows that proteins not involved in amyloidoses, are able to form, in vitro, amyloid-like prefibrillar and fibrillar assemblies indistinguishable from those grown from proteins associated with disease. Previous studies showed that early prefibrillar aggregates of the N-terminal domain of the prokaryotic hydrogenase maturation factor HypF (HypF-N) are cytotoxic, inducing early mitochondria membrane depolarization, activation of caspase 9 and eventually cell death. To gain knowledge on the molecular basis of HypF-N aggregate cytotoxicity, we performed a differential proteomic analysis of NIH-3T3 cells exposed to HypF-N prefibrillar aggregates in comparison with control cells. Two-dimensional gel electrophoresis followed by protein identification by MALDI-TOF MS, allowed us to identify 21 proteins differentially expressed. The changes of the expression level of proteins involved in stress response (Hsp60 and 78 kDa glucose-regulated protein) and in signal transduction (Focal adhesion kinase1) appear particularly interesting as possible determinants of the cell fate. The levels of some of the differently expressed proteins were modified also in similar studies carried out on cells exposed to Aβ or α-synuclein aggregates, supporting the existence of shared features of amyloid cytotoxicity.

1. Introduction

Amyloid diseases are a group of protein misfolding pathologies including either systemic forms (i.e. type II diabetes mellitus,) and neurodegenerative diseases (Alzheimer's, Parkinson's, Huntington and prion diseases) (reviewed in [1,2]). The molecular basis of these clinically different pathologies can be traced back to the presence, in the affected tissues and organs, of proteinaceous deposits of fibrillar aggregates of one out of a number of peptides or proteins, each found aggregated specifically in each disease (reviewed in [1,3]). In the last ten years it has became increasingly clear that the ability to oligomerize into amyloid assemblies is not a specific feature of the proteins and peptides found aggregated in tissues affected by amyloid diseases; in fact, since 1998, an increasing number of reports support the idea that protein misfolding following mutations, chemical modifications, presence of destabilizing surfaces or any other alteration of the chemical environment, can result a structural reorganization, favouring oligomerization/polymerization of peptides and proteins into amyloids [4,5].

In addition to amyloid aggregation, aggregate toxicity has also recently resulted as a generic property of proteins and peptides. In particular, it is increasingly recognized that amyloid oligomers, preceding the appearance of mature fibrils, known as prefibrillar aggregates, are the most toxic species, among amyloid assemblies associated or not associated with disease [6,7]. This view supports the idea that any protein can potentially become the source of toxic species impairing cell viability and that the cytotoxicity of prefibrillar aggregates results, at least in part, from shared basic structural features of the latter [8]. Moreover, a growing number of studies suggest that, in most cases, the cell membrane, can also favour protein/peptide misfolding favouring the appearance of aggregating nuclei [9]. Conversely, toxic prefibrillar aggregates from disease-associated or disease-unrelated proteins can interact with the cell membranes modifying their structural order resulting in the early impairment of ion and redox homeostasis [10,11]. Intense efforts are presently dedicated at unravelling the molecular basis of the appearance in tissue of protein aggregates and their cytotoxicity. However, much must still be learnt to gain enough knowledge to allow designing therapeutic strategies aimed at counteracting the clinical symptoms of amyloid diseases. On this respect, it can be important to investigate the cytotoxic effects on cells exposed to amyloid aggregates of proteins/peptides not associated with any amyloid

Abbreviations: 2D-GE, two dimensional gel electrophoresis; IEF, isoelectrofocusing; MS, mass spectrometry; MALDI-TOF, matrix assisted laser desorption/ionization time-of-flight; LC-MS/MS, liquid chromatography, tandem mass spectrometry; CHAPS, 3-[(3cholamidopropyl)dimethylammonio]-1-propanesulfonic acid; ECL, Enhanced Chemiluminescence; HypF-N, hydrogenase maturation factor; HypF-N, N-terminal domain of the prokaryotic hydrogenase maturation factor HypF

* Corresponding author.
E-mail address: Francesca.magherini@unifi.it (F. Magherini).

1570-9639/$ – see front matter © 2009 Elsevier B.V. All rights reserved.
doi:10.1016/j.bbapap.2009.04.009

disease. Such study can highlight cell modifications resulting from shared structural features in amyloids excluding those associated with the specific features of any aggregated peptide/protein.

The advent of proteomics has allowed the simultaneous analysis of changes in the expression pattern of multiple proteins in complex biological systems. This appears particularly important in the case of cell dysfunctions resulting from protein aggregation. The effects protein aggregates have on cells appear highly complex and heterogeneous. Such a complex pattern of cell impairment makes proteomics one of the most useful tools to integrate these modifications into a whole systematic picture. The reports that recently appeared on the proteomic analysis of amyloid diseases such as Alzheimer's disease, Parkinson's disease and others have provided valuable data on some cell modifications allowing to explain, at least in part, cell impairment in these diseases [12–16]. Proteomic studies provided useful information on the changes in pattern of protein expression in cells exposed to toxic aggregates of specific peptides/proteins found aggregated in the corresponding diseases.

In the present study we performed a proteomic analysis of NIH-3T3 cells exposed to toxic aggregates of a protein domain not involved in any amyloid disease, the N-terminal domain of the prokaryotic HypF hydrogenase maturation factor (HypF-N) whose aggregation properties and aggregate cytotoxicity were previously characterized [8,10,17]. To our knowledge, this is the first proteomic study on the alterations of the protein expression profiles in cells exposed to toxic amyloid aggregates of a disease-unrelated protein.

Our results highlight some generic changes in protein expression pattern elicited by the shared features of amyloids such as the basic cross-beta structure and the exposure of hydrophobic patches. We found significant differences in the protein expression patterns in the exposed cells, with a number of up- or down-regulated proteins. Some of these proteins were also found in similar studies carried out on cells exposed to Aβ or α-synuclein aggregates in agreement with the generic nature of the cellular changes underlying amyloid cytotoxicity. Among the differentially expressed proteins, the reduced expression of Fak1 observed in the exposed cells can be related to the apoptotic process, whereas the increased expression of Hsp60 can provide protection against cell stress induced by HypF-N prefibrillar aggregates. Furthermore the treated cells showed a marked increase of the expression of both glyceraldehyde 3-phosphate dehydrogenase (Gapdh) and enolase. These two proteins are involved in energy metabolism and Gapdh has also been shown to bind the β-amyloid precursor protein [18] and to be involved in transcriptional regulation of cell-cycle [19]. Finally, we observed an increase in the expression level of actin as previously shown in cell exposed to the intracellular domain of the β-amyloid precursor protein [20].

2. Materials and Methods

2.1. HypF-N expression and purification

HypF-N was expressed and purified as previously described [17]. HypF-N prefibrillar aggregates were obtained by incubating the protein for 48 h at room temperature at a concentration of 0.3 mg/ml in 30% (v/v) trifluoroethanol, 50 mM sodium acetate, 2 mM dithiotreitol (DTT), pH 5.5, as previously reported [17]. At the end of the incubation the solution was centrifuged, and the resulting pellet was dried under N_2 to remove the residual solvent, dissolved in DMEM at 200 μM (monomeric protein concentration) and immediately added to the cell culture medium at 2 μM final concentration.

2.2. Cell culture and treatment

Cell culture media and other reagents, unless otherwise stated, were from Sigma-Aldrich Fine Chemicals Co. NIH-3T3 murine fibroblasts (ATCC, Manassas, VA) were routinely cultured in Dulbecco's modified Eagle's medium (DMEM) with 4.5 g/l glucose, containing 10% bovine calf serum (HyClone Lab, Perbio Company, Celbio), 3 mM glutamine, 100 U/ml penicillin and 100 μg/ml streptomycin, in a 5% CO_2 humidified environment at 37 °C. Cells were used for a maximum of 10 passages. Sub-confluent NIH-3T3 cells were treated for differing lengths of time with 2 μM toxic HypF-N prefibrillar aggregates. Under these conditions it was previously shown that the aggregates are stable in the culture media [8]. Controls were performed by exposing the cells to the same amount of native, soluble HypF-N. At the end of each treatment, the cells were washed twice with phosphate-buffered saline (PBS), dried and stored at −80 °C.

2.3. Sample preparation and 2D-GE

Cells were scraped in RIPA buffer (50 mM Tris–HCl pH 7.0, 1% NP-40, 150 mM NaCl, 2 mM EGTA, 100 mM NaF) containing a cocktail of protease inhibitors (Sigma). The cells were sonicated (10 s) and protein extracts were clarified by centrifugation at 8000 *g* for 10 min. Proteins were precipitated following a chloroform/methanol protocol [21] and the pellet was resuspended in 8 M urea, 4% CHAPS and 20 mM DTT. Three independent experiments were performed and each sample was run in triplicate in order to assess biological and analytical variation. IEF (first dimension) was carried out on non-linear wide-range immobilized pH gradients (pH 3.0–10; 18 cm long IPG strips; GE Healthcare, Uppsala, Sweden) and achieved using the Ettan™ IPGphor™ system (GE Healthcare, Uppsala, Sweden). Analytical-run IPG strips were rehydrated with 60 μg of total proteins in 350 μl of lysis buffer and 0.2% carrier ampholyte for 1 h at 0 V and for 8 h at 30 V, at 20 °C. MS-preparative IPG strips were loaded with 400 μg of proteins. The strips were focused at 20 °C according to the following electrical conditions: 200 V for 1 h, from 300 V to 3500 V in 30 min, 3500 V for 3 h, from 3500 V to 8000 V in 30 min, and 8000 V until a total of 80,000 V/h was reached. After focusing, analytical and preparative IPG strips were equilibrated for 12 min in 6 M urea, 30% glycerol, 2% SDS, 2% DTT in 0.05 M Tris–HCl buffer, pH 6.8, and subsequently for 5 min in the same urea/SDS/Tris buffer solution where DTT was substituted with 2.5% iodoacetamide. The second dimension was carried out on 9–16% polyacrylamide linear gradient gels (18 cm × 20 cm × 1.5 mm) at 10 °C and 40 mA/gel constant current until the dye front reached the bottom of the gel. Analytical gels were stained with ammoniacal silver nitrate as previously described [22]; MS-preparative gels were stained with colloidal Coomassie [23].

2.4. Western blotting analysis of proteomic candidates

For 1-DE 30 μg of protein extracts was separated by 12% SDS-PAGE and transferred onto a PVDF membrane (Millipore). To confirm the results obtained from 2D-GE analysis, the relative amount of Hsp60 and Fak proteins were assessed by Western blot with appropriate antibodies (Santacruz). For quantification, the blots were stained with Coomassie brilliant blue R-250 and subjected to densitometric analysis performed using Quantity One Software (Bio-Rad). Statistical analysis of the data was performed by Student's *t*-test; *p*-values 0.05 were considered statistically significant. The intensity of the immunostained bands were normalized with the total protein intensities measured by Coomassie brilliant blue R-250 from the same blot.

2.5. Image analysis and statistics

The gel and Western blot images were acquired with an Epson expression 1680 PRO scanner. For each condition, three biological replicates were performed and only the spots present in all the replicates were taken in consideration for subsequent analysis. Computer-aided 2D image analysis was carried out using ImageMaster 2-DE Platinum software version 6.0 (GE Healthcare). The

relative spot volume calculated as %*V* (*V* single spot/*V* total spots, where *V* = integration of OD over the spot area) was used for quantitative analysis in order to decrease experimental errors. The normalized intensity of the spots on replicate 2D gels was averaged and standard deviation was calculated for each condition. A two-tiled non paired Student's *t*-test was performed using ORIGIN 6.0 (Microcal Software, Inc.) to determine whether the relative change was statistically significant.

2.6. In-gel trypsin digestion and MALDI-TOF mass spectrometry

The analysis was performed on the Coomassie blue-stained spots excised from the gels. The spots were washed first with acetonitrile and then with 0.1 M ammonium bicarbonate. Protein samples were reduced by incubation in 10 mM dithiothreitol (DTT) for 45 min at 56 °C. The cysteines were alkylated by incubation in 5 mM iodoacetamide for 15 min at room temperature in the dark. The gel particles were then washed with ammonium bicarbonate and acetonitrile. Enzymatic digestion was carried out with trypsin (12.5 ng/μl) in 50 mM ammonium bicarbonate buffer, pH 8.5, at 4 °C for 4 h. The buffer solution was then removed and a new aliquot of the enzyme/buffer solution was added for 18 h at 37 °C. A minimum reaction volume, enough for complete gel rehydration was used. At the end of the incubation the peptides were extracted by washing the gel particles with 20 mM ammonium bicarbonate and 0.1% TFA in 50% acetonitrile at room temperature and then lyophilised. Positive Reflectron MALDI spectra were recorded on a Voyager DE STR instrument (Applied Biosystems, Framingham, MA). The MALDI matrix was prepared by dissolving 10 mg of alpha cyano in 1 ml of acetonitrile/water (90:10 v/v). Typically, 1 μl of matrix was applied to the metallic sample plate and then 1 μl of analyte was added. Acceleration and reflector voltages were set up as follows: target voltage at 20 kV, first grid at 70% of target voltage, delayed extraction at 100 ns to obtain the best signal-to-noise ratios and the best possible isotopic resolution with multipoint external calibration using a peptide mixture purchased from Applied Biosystems. Each spectrum represents the sum of 1500 laser pulses from randomly chosen spots per sample position. Raw data were analyzed using the computer software provided by the manufacturers and are reported as monoisotopic masses.

2.7. nanoLC mass spectrometry

A mixture of peptide solution was subjected to LC-MS analysis using a 4000Q-Trap (Applied Biosystems) coupled to an 1100 nano HPLC system (Agilent Technologies). The mixture was loaded on an Agilent reverse-phase pre-column cartridge (Zorbax 300 SB-C18, 5×0.3 mm, 5 μm) at 10 μl/min (A solvent 0.1% formic acid, loading time 5 min). The peptides were separated on an Agilent reverse-phase column (Zorbax 300 SB-C18, 150 mm×75 μm, 3.5 μm), at a flow rate of 0.3 μl/min with a 0% to 65% linear gradient in 60 min (A solvent 0.1% formic acid, 2% acetonitrile in MQ water; B solvent 0.1% formic acid, 2% MQ water in acetonitrile). Nanospray source was used at 2.5 kV with liquid coupling, with a declustering potential of 20 V, using an uncoated silica tip from NewObjectives (O.D. 150 μm, I.D. 20 μm, T.D. 10 μm). The data were acquired in information-dependent acquisition (IDA) mode, in which a full scan mass spectrum was followed by MS/MS of the 5 most abundant ions (2 s each). In particular, spectra acquisition of MS-MS analysis was based on a survey Enhanced MS Scan (EMS) from 400 m/z to 1400 m/z at 4000 amu/s. This scan mode was followed by an Enhanced Resolution experiment (ER) for the five most intense ions and then MS2 spectra (EPI) were acquired using the best collision energy calculated on the basis of m/z values and charge state (rolling collision energy) from 100 m/z to 1400 m/z at 4000 amu/s. The data were acquired and processed using the Analyst software (Applied Biosystems).

2.8. MASCOT analysis

The spectral data were analyzed using the Analyst software (version 1.4.1) and the MS-MS centroid peak lists were generated using the MASCOT.dll script (version 1.6b9). The MS-MS centroid peaks were threshold at 0.1% of the base peak. MS-MS spectra with less than 10 peaks were rejected. The spectra were searched against the Swiss Prot database (2006.10.17 version) using the licensed version of Mascot 2.1 (Matrix Science), after converting the acquired MS-MS spectra in MASCOT generic file format. The MASCOT search parameters were: taxonomy mus musculus; allowed number of missed cleavages 2; enzyme trypsin; variable post-translational modifications, methionine oxidation, pyro-glu N-term Q; peptide tolerance 200 ppm and MS/MS tolerance 0.6 Da; peptide charge, from +2 to +3 and top 20 protein entries. Spectra with a MASCOT score <25 having low quality were rejected. The score used to evaluate the quality of matches for the MS-MS data was higher than 30. However, the spectral data were manually validated and contained sufficient information to assign peptide sequence.

3. Results

3.1. Comparative proteomic analysis between control cells and cells exposed to HypF-N prefibrillar aggregates

Previous experiments performed by Bucciantini et al. showed that prefibrillar HypF-N aggregates induced early Ca^{2+} increase and oxidative stress followed by mitochondria depolarization and caspase activation in exposed NIH-3T3 cells. After 24 h, the cells died with necrotic features possibly since the ATP levels were too low to sustain the initially triggered apoptotic program [10]. In order to investigate the changes (if any) in protein expression induced in the same cells upon exposure to HypF-N prefibrillar aggregates, we performed a 2D-GE followed by mass spectrometry. In all the experiments carried out in this study, the cells were exposed to 2 μM prefibrillar aggregates. This protein concentration was chosen to investigate finely regulated biochemical processes, such as the activation of pro-apoptotic factors, which could be hidden by a stronger cell injury [10]. The cells were treated for 5 and 24 h and proteins extracts were prepared as described under Materials and methods. Then the proteins were separated by 2D-GE and the resulting silver-stained gels were analyzed using the ImageMaster 2D Platinum 6.0 software. The differences of protein expression between control and treated cells were taken into consideration if the relative volume of the spots differed reproducibly more than 1.5-fold and this difference was statistically significant. An average of about 1300 spots was detected in each silver-stained gel. Cell exposure to HypF-N prefibrillar aggregates did not affect the overall proteomic profiles both after 5 h and after 24 h (Figs. 1 and 2). However, the computer analysis highlighted 19 variations between cells treated for 5 h with 2 μM HypF-N prefibrillar aggregates (Fig. 1B) and the control cells treated for the same length of time with an equivalent amount of native HypF-N (Fig. 1A). Among these variations, only two were still present after 24 h of treatment with aggregates (Fig. 2) indicating that the alteration of the expression is a transient event, at least for this group of proteins, except two. On the other hand, the comparison between cells treated for 24 h with 2 μM HypF-N prefibrillar aggregates and control cells showed a variation of 9 spots, whose expression was not affected after 5 h, indicating that some proteins are up- or down-regulated as a consequence of the prolonged exposure to the aggregates.

3.2. Identification of differentially expressed proteins

In order to identify the proteins of interest, 400 μg of protein lysates was loaded on preparative gels and stained with colloidal

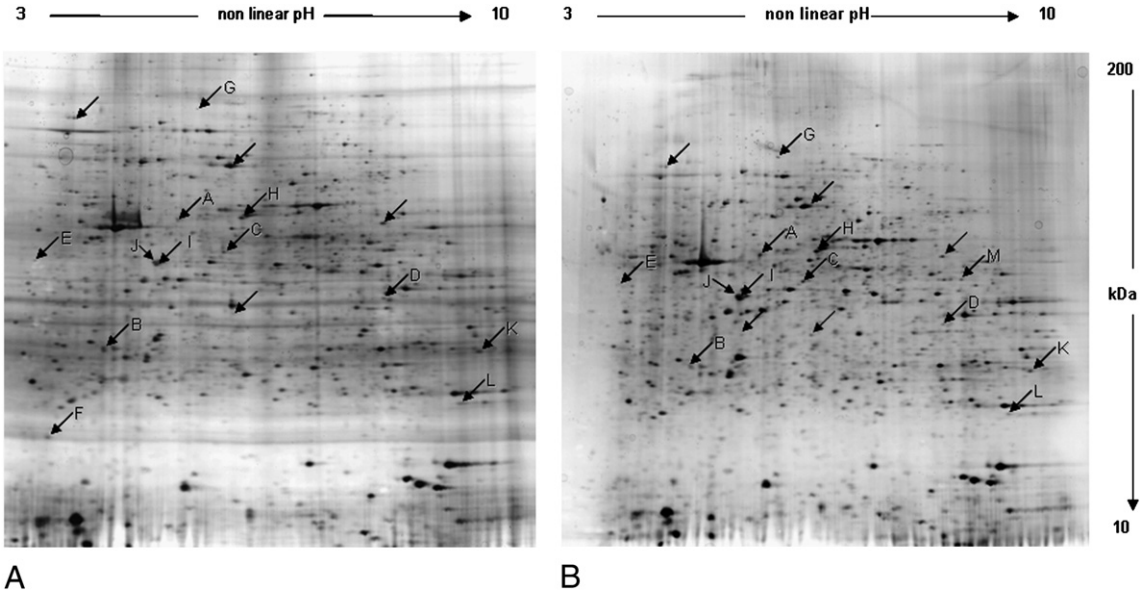

Fig. 1. 2D images of silver stained gels of total proteins extracted from control and HypF-N prefibrillar aggregate treated cells for 5 h. Arrows indicate variations between control (panel A) and treated cells (panel B). Letters indicate the identified proteins. Controls were performed by exposing the cells to native, soluble HypF-N.

Coomassie. The spots indicated by arrows in representative gels shown in Figs. 1 and 2 were selected for mass spectral identification after merging the images of preparative and analytical gels. The proteins excised from the gels were reduced, alkylated and in situ digested with trypsin. The resulting peptide mixtures were directly analyzed by MALDI/MS according to the peptide mass fingerprinting procedure. The peaks detected in the MALDI spectra were used to search for a non redundant sequence database using the in house MASCOT software, taking advantage of the specificity of trypsin and the taxonomic category of the samples. The number of measured masses that matched within the given mass accuracy of 200 ppm was recorded and the proteins that received the highest number of peptide matches were examined. Some spots could not be identified unambiguously either due to the low protein content of the spot or to the presence of more than one protein per spot. Among the 19 spots differentially expressed after 5 h of cell exposure to the aggregates, 13 spots were successfully identified and are indicated by arrows and letters in Fig. 1. Among the 9 spots differentially expressed in cells treated for 24 h with 2 μM HypF-N prefibrillar aggregates, 8 spots were identified and are indicated by arrows and numbers in Fig. 2. Some spots gave no confident identification by the peptide mass fingerprinting procedure. Additional data were then provided by nanoLC/MS/MS experiments. The peptide mixtures were fractionated by nanoHPLC and sequenced by tandem mass spectrometry leading to the unambiguous identification of the protein candidate. The lists of proteins identified by these approaches are reported in Table 1 (5 h treatment) and in Table 2 (24 h treatment). The identified proteins included cytoskeleton elements (actin, tubulin alpha 1C chain, microtubule-actin cross-linking factor 1), enzymes involved in energy metabolism and transcriptional regulation (Gapdh, enolase), proteins involved in stress response (Hsp60 and 78 kDa glucose-regulated protein) and the focal adhesion kinase, Fak1. Among these proteins only Fak1 and Hsp60 showed an

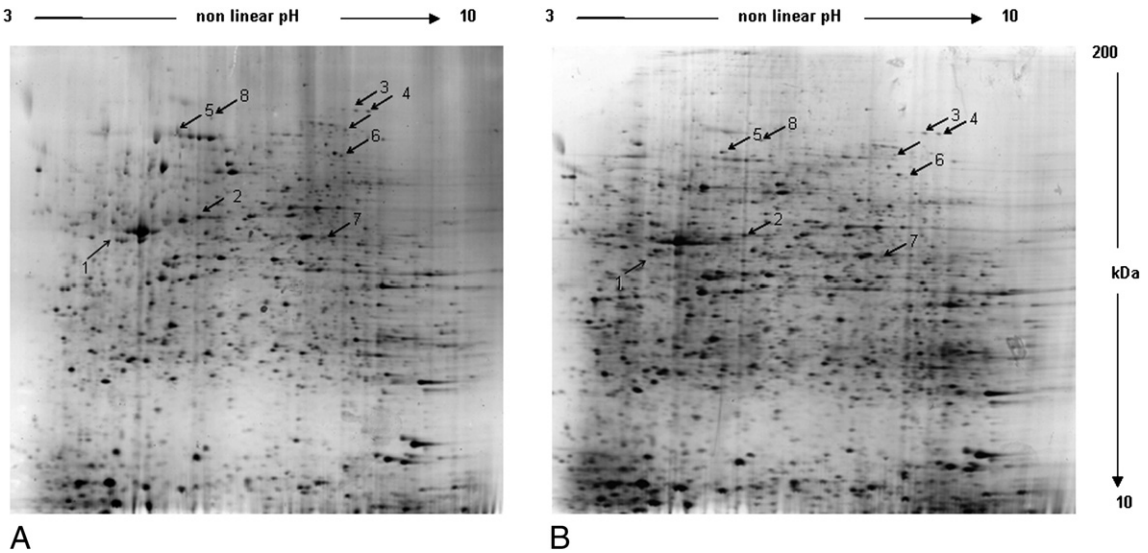

Fig. 2. 2D images of silver stained gels of total proteins extracted from control and HypF-N prefibrillar aggregate treated cells for 24 h. Arrows indicate variations between control (panel A) and treated cells (panel B). Numbers indicate the identified proteins. Controls were performed by exposing the cells to native, soluble HypF-N.

Table 1
Relative change in protein expression in cells treated for 5 h with HypF-N prefibrillar aggregates versus control cells.

Spot	Protein name	Accession number	MASCOT score	No. of matched peptides	Sequence coverage (%)	Fold change	*p*-value	Functional categorization
Up-regulated by HypF-N								
A	Hsp60	P63038	162	5	12%	+1.58	0.0005	Protein folding and stress response
B	Actin	P60710	79	5	22%	Only in treated cells.	N.D.	Cytoskeletal organization
C	Actin	P60710	241	7	18%	+9.8	0.007	Cytoskeletal organization
D	Glyceraldehyde-3-phosphate dehydrogenase	P16858	120	7	33%	+9.7	0.0081	Energy related (glycolysis)
E	78 kDa glucose-regulated protein	P20029	78	2	5%	+4.8	0.1	Protein folding and stress response (response to unfolded proteins)
F	Nucleophosmin	Q61937	165	5	15%	Only in treated cells.	N.D.	Associated with nucleolar ribonucleoprotein structures and bind single-stranded nucleic acids
Down-regulated by HypF-N								
G	Focal Adhesion kinase-1	P34152	77	17	22%	−1.6	0.01	Non-receptor protein-tyrosine kinase involved in cell motility. Proliferation and apoptosis.
H	Enolasi-1	P17182	118	12	32%	−2.4	0.09	Energy related (glycolysis)
I	Tubulin alpha-1C chain	P68373	80	9	31%	−8.3	0.015	Major constituent of microtubules
J	Annexin-A3	O35639	111	13	43%	−2	0.019	Inhibitor of phospholipase A2
K	Hsp60	P63038	85	2	5%	−1.6	0.032	Protein folding and stress response
L	Transgelin-2	Q9WVA4	171	7	41%	Only in control cells	N.D.	Belongs to the calponin family
M	Heparan sulfate glucosamine 3-O-sulfotransferase 2	Q673U1	47	2	4%	Only in control cells	N.D.	Catalyzes the O-sulfation of glucosamine

expression variation persisting over time, since it was observed both after 5 and after 24 h of cell exposure to the aggregates.

3.3. Validation of proteomics results

In order to validate the proteomic results, the amounts of Fak1 and Hsp60 were evaluated by Western blot analysis with specific antibodies as shown in Fig. 3, panels A and B, respectively. Thirty μg of proteins was loaded on 12% SDS-PAGE and transferred onto a PVDF membrane. For quantification, the intensities of the immunostained bands were normalized to the total protein intensities in the same blot, as measured by Coomassie brilliant blue. In Fig. 3, panel C the histograms representing the variation of the expression of Fak1 and Hsp60 are also reported. Such analysis confirmed the decrease of Fak1 expression and the increase of Hsp60 expression both after 5.0 and 24 h.

3.4. Protein expression changes in cells exposed for 5 h to HypF-N prefibrillar aggregates

In cells exposed to HypF-N prefibrillar aggregates for 5 h, 6 spots (A to F in Table 1) appeared up-regulated, whereas 7 spots (G to M in Table 1) appeared down-regulated. Among the up-regulated proteins, we found the heat shock protein Hsp60 (spot A). Hsp60 belongs to a family of highly homologous chaperone proteins that are induced in response to environmental, physical and chemical stresses, including accumulations of misfolded proteins and reactive oxygen species [24,25]. The increase of Hsp60 expression limits the consequences of damage facilitating cell recovery. Hsp60 was also identified in the spot K, which was down-regulated upon cell treatment with the aggregates. However, the position in the gel and the peptide coverage, indicates that this spot is probably a fragment arising from a proteolytic cleavage of Hsp60.

A further indication of a stress condition induced in cells exposed to the HypF-N aggregates is the marked increase in the expression of the key glycolytic enzyme Gapdh (spot D). This protein plays a central role in glycolysis, catalyzing the reversible conversion of glyceraldehyde-3-phosphate to 1,3-bisphosphoglycerate. More recent studies have highlighted unexpected non-glycolytic functions of Gapdh in physiological and pathological processes, including transcriptional regulation of cell-cycle [19]. In addition two spots corresponding to actin were up-regulated. Among the proteins whose expression appeared decreased upon exposure to HypF-N prefibrillar aggregates, the focal adhesion kinase (Fak1; spot G) is particularly interesting.

Table 2
Relative change in protein expression in cells treated for 24 h with HypF-N prefibrillar aggregates versus control cells.

Spot	Protein name	Accession number	MASCOT score	No. of matched peptides	Sequence coverage (%)	Fold change	*p*-value	Functional categorization
Up-regulated by HypF-N								
1	Ovostatin homolog	Q3UU35	48	4	15%	+1.4	0.028	Proteases inhibitor
2	Hsp60	P63038	162	5	12%	+1.58	0.0005	Protein folding and stress response
Down-regulated by HypF-N								
3	Microtubule-actin cross-linking factor 1	Q9QXZ0	82	14	10%	−1.66	0.035	F-actin-binding protein which may play a role in cross-linking actin to other cytoskeletal proteins
4	Microtubule-actin cross-linking factor	Q9QXZ0	88	10	8%	−2.24	0.023	
5	Pol protein	Q7M6W3	73	10	17%	−1.67	0.1	Unknown
6	Pdia2 protein	Q14AV9	43	2	5%	−3.21	0.004	Protein disulfide isomerase
7	Poly(rC)-binding protein 2	Q61990	71	2	6%	−3.78	0.014	Single-stranded nucleic acid binding protein
8	Fak1 focal adhesion kinase	P34152	77	17	22%	−1.53	0.015	Non-receptor protein-tyrosine kinase involved in cell motility, proliferation and apoptosis

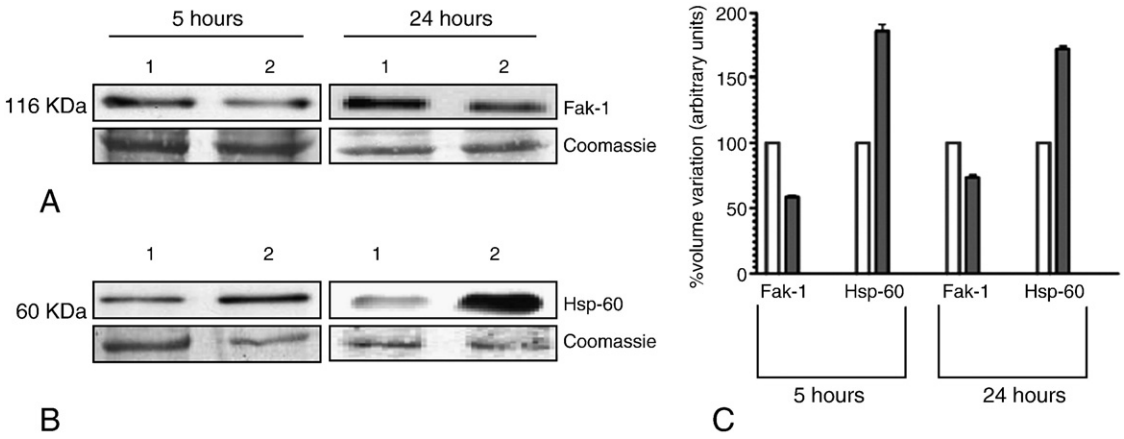

Fig. 3. Validation of proteomic results by western blot analysis. Western blot were probed with antibodies against Fak1 and Hsp60 proteins identified by proteomic screening. The intensity of immunostained bands was normalized with the total protein intensities measured from the same blot stained with Coomassie brilliant blue (in panel A and panel B a representative band of the lane is reported). (A) Aggregate-induced reduced expression of Fak1 after 5 and 24 h of treatment: lane 1, cells exposed to native HypF-N; lane 2, cells exposed to HypF-N prefibrillar aggregates. (B) Aggregate-induced increased expression of Hsp60 after 5 and 24 h of treatment: lane 1, cells exposed to native HypF-N; lane 2, cells exposed to HypF-N prefibrillar aggregates. (C) Histograms representing Fak1 and Hsp60 protein expression variation. The two-tailed non paired Student's *t*-test was performed using ORIGIN 6.0. ($p<0.05$).

Fak1 is a non-receptor cytoplasmic tyrosine kinase that plays a key role in the regulation of proliferation and migration of normal and tumour cells [26, 27]. Interestingly, Fak1 and Hsp60 are the only two proteins, among those differentially expressed after 5 h of cell exposure, that do not recover a normal expression level after 24 h.

3.5. Protein expression changes in cells exposed for 24 h to HypF-N prefibrillar aggregates

It was previously shown that NIH-3T3 cells treated for 24 h with 10 μM HypF-N prefibrillar aggregates die with necrotic features, including cytoplasmic vacuolization and nuclear swelling after an initial apoptotic activation [10]. The amount of HypF-N aggregates (2 μM, soluble protein concentration) used in this work is not so high to induce cell death, thus allowing the cells to overcome damage. After 24 h of cell exposure to HypF-N aggregates, few other proteins, besides Fak1 and Hsp60, displayed altered expression. In particular, we identified 6 new spots (1 up-regulated and 5 down-regulated). Among the proteins down-regulated, the microtubule-actin cross-linking factor 1 (MACF1, spot 3) belongs to the Plakin family, that includes proteins involved in the linkage of cytoskeletal elements and the junctional complex. MACF1 was found to regulate microtubule remodelling in response to the activation of signal transduction pathways, although its function has not yet been fully explored [28, 29].

4. Discussion

To our knowledge, this study is the first proteomic investigation focused on highlighting the alterations of the protein expression profiles in a cultured cell model exposed to toxic amyloid aggregates of a protein not involved in any amyloid disease. Our analysis was performed using a non lethal dose of HypF-N prefibrillar aggregates, allowing the detection of fine variations more directly implicated in a response to the cell injury given by the aggregates, instead of the complex pattern of changes arising during the process of cell death.

Our approach led us to identify a subset of cell proteins whose levels were significantly altered upon cell exposure to the aggregates for 5 h or 24 h. Some of the proteins detected in our investigation, including Hsp60, actin, enolase-1 and Gapdh had previously been identified in other proteomic studies carried out on cells exposed to Aβ42 or α-synuclein. In Table 3 a comparison between the protein identified in our study and the proteins identified in other studies is shown, indicating that there is a general response of cells to toxic aggregates that is not sequence specific [12,13,30,31,32]. Actually, changes in the expression levels of Gapdh, actin, tubulin and heat shock proteins have frequently

Table 3
Protein expression changes observed in this study in comparison to previous protein reported in other studies.

Protein	Amyloid aggregates	Cell type or animal model	
GAPDH	HypF-N	NIH3T3 fibroblast cells	This study
	Amyloid β-peptide	Mitochondria from primary neuron	[30]
		Tg2576 transgenic mice	[31]
		3xTgAD Alzheimer's mice (hippocampal protein)	[12]
	β-amyloid (1–42)	P301L tau overexpressing SH-SY5Y	[32]
Tubulin α-chain	HypF-N	NIH3T3 fibroblast cells	This study
	β-amyloid (1–42)	SN56.B5.G4 cholinergic cells	[13]
		3xTgAD Alzheimer's mice (hippocampal protein)	[12]
	β-amyloid (1–42)	Amygdalae from P301L tau transgenic mice	[32]
78 kDa glucose-regulated protein	HypF-N	NIH3T3 fibroblast cells	This study
		3xTgAD Alzheimer's mice (hippocampal protein)	[12]
	β-amyloid (1–42)	P301L tau overexpressing SH-SY5Y	[32]
Enolase	HypF-N	NIH3T3 fibroblast cells	This study
		Tg2576 transgenic mice	[31]
		3xTgAD Alzheimer's mice (hippocampal protein)	[12]
Hsp60		3xTgAD Alzheimer's mice	[12]
Actin	HypF-N	NIH3T3 fibroblast cells	This study
	β-amyloid (1–42)	Amygdalae from P301L tau transgenic mice	[32]

been reported in amyloid-linked proteomic studies possibly because they are related to a generic response to stress conditions [33] such as that associated with the growth of amyloid aggregates. In our experiments, cell exposure to toxic amyloid aggregates induced an increase of the expression levels of several proteins such as Hsp60. In addition to its chaperone activity, Hsp60 has been suggested to perform complex functions, producing both anti- and pro-apoptotic effects. In fact, cytosolic Hsp60, can promote either cell survival or caspase-mediated cell death by preventing the translocation of the pro-apoptotic protein Bax into the mitochondria or by favouring the maturation of procaspase-3, respectively [34–38]. In a recent study, Hsp60, Hsp70, and Hsp90 were shown to provide differential protection against intracellular stress caused by β-amyloid by maintaining the efficiency of the mitochondrial oxidative phosphorylation and the tricarboxylic acid cycle enzymes. In particular, Hsp60 was shown to prevent the inhibition of complex IV activity by β-amyloid, thus preventing apoptosis [39].

We also found significantly increased levels of Gapdh and actin. As far as Gapdh is concerned, several recent studies have shown that, in addition to glycolysis, it is involved in several glycolysis-unrelated activities; these include a role in vesicle fusion and transport [40], microtubule bundling [41], nuclear RNA transport [42], and transcription [43]. Furthermore, increased expression and nuclear translocation of Gapdh have recently been reported to participate to the apoptotic pathway in different cell types [44–47]. Finally, Gapdh has also been reported to bind to a variety of proteins involved in neuronal diseases, including the amyloid precursor protein and huntingtin [18]. The increased levels of actin expression in cells exposed to prefibrillar HypF-N aggregates are similar to the effects previously reported by Muller et al.; these authors found up-regulation of the actin gene expression in cells harbouring the cytoplasmic domain of the amyloid precursor protein [20].

Finally, we found a significant decrease of Fak1 in cells exposed both 5 h and 24 h to the HypF-N aggregates. The repression of Fak1 synthesis in exposed cells, confirmed by Western blot analysis, is one of the major results of this proteomic analysis. In vivo animal studies have shown that Fak1 expression is increased in a number of human cancers, thus contributing to tumour development and malignancy [48]. Moreover, Fak1 has recently been shown to be a critical protein in survival signalling, since it blocks apoptosis induced by several stimuli [49]. Fak1 expression decrease following proteolytic cleavage in various cell types has been associated with various cell dysfunctions including c-Myc-induced apoptosis of chicken embryo fibroblasts (CEF) [49], growth factor deprivation-induced apoptosis of human umbilical vein endothelial cells [50], and detachment-induced cell death (anoikis) of intestinal epithelial cells [51]. In a recent study, different epithelial cell lines treated with thimerosal displayed increased levels of hydrogen peroxide resulting in caspase activation, Fak1 cleavage and apoptosis [52]. All these observations suggest that the decreased Fak1 expression in NIH-3T3 cells treated with HypF-N aggregates could be related to the apoptotic process: in particular its decreased intracellular levels could be the consequence of a proteolytic cleavage making the cells more vulnerable to death.

The reported changes in protein expression profiles in exposed cells suggest some alterations in specific signalling pathways involved in the control of gene transcription and translation and/or in protein degradation pathways. These alterations could be triggered, at least in part, by modifications of signalling pathways following the reported interaction of amyloid aggregates with the cell membrane [10, 11, 53]. Overall, our results can provide useful information on the crucial events underlying cytotoxicity induced by amyloid aggregates of different peptides or proteins both related and unrelated to disease.

Acknowledgements

This work was supported by grants from the INBB, the Italian Ministero dell'Universita` e della Ricerca Scientifica (PRIN 2006 and 2007) and the Ente Cassa di Risparmio di Firenze. Support from the National Center of Excellence in Molecular Medicine (MIUR — Rome) and from the Regional Center of Competence (CRdC ATIBB, Regione Campania — Naples) is gratefully acknowledged.

References

[1] M. Stefani, C.M. Dobson, Protein aggregation and aggregate toxicity: new insights into protein folding, misfolding diseases and biological evolution, J. Mol. Med. 81 (2003) 678–699.
[2] M. Stefani, Protein misfolding and aggregation: new examples in medicine and biology of the dark side of the protein world, Biochim. Biophys. Acta 1739 (2004) 5–25.
[3] F. Chiti, C.M. Dobson, Protein misfolding, functional amyloid, and human disease, Annu. Rev. Biochem. 75 (2006) 333–366.
[4] J.I. Guijarro, M. Sunde, J.A. Jones, I.D. Campbell, C.M. Dobson, Amyloid fibril formation by an SH3 domain, Proc. Natl. Acad. Sci. U. S. A. 95 (1998) 4224–4228.
[5] F. Chiti, P. Webster, N. Taddei, A. Clark, M. Stefani, G. Ramponi, C.M. Dobson, Designing conditions for in vitro formation of amyloid protofilaments and fibrils, Proc. Natl. Acad. Sci. U. S. A. 96 (1999) 3590–3594.
[6] C.G. Glabe, Common mechanisms of amyloid oligomer pathogenesis in degenerative diseases, Neurobiol. Aging 27 (2006) 570–575.
[7] C.G. Glabe, R. Kayed, Common structure and toxic function of amyloid oligomers implies a common mechanism of pathogenesis, Neurology 66 (2006) 74–78.
[8] M. Bucciantini, G. Calloni, F. Chiti, L. Formigli, D. Nosi, C.M. Dobson, M. Stefani, Prefibrillar amyloid protein aggregates share common features of cytotoxicity, J. Biol. Chem. 279 (2004) 31374–31382.
[9] M. Zhu, P.O. Souillac, C. Ionescu-Zanetti, S.A. Carter, A.I. Fink, Surface-catalyzed amyloid fibril formation, J. Biol. Chem. 277 (2002) 50914–50922.
[10] M. Bucciantini, S. Rigacci, A. Berti, L. Pieri, C. Cecchi, D. Nosi, L. Formigli, F. Chiti, M. Stefani, Patterns of cell death triggered in two different cell lines by HypF-N prefibrillar aggregates, FASEB J. 19 (2005) 437–439.
[11] J.I. Kourie, Mechanisms of amyloid beta protein-induced modification in ion transport systems: implications for neurodegenerative diseases, Cell. Mol. Neurobiol. 21 (2001) 173–213.
[12] B. Martin, R. Brenneman, K.G. Becker, M. Gucek, R.N. Cole, S. Maudsley, iTRAQ analysis of complex proteome alterations in 3xTgAD Alzheimer's mice: understanding the interface between physiology and disease, PLoS ONE 23 (2008) e2750.
[13] S. Joerchel, M. Raap, M. Bigl, K. Eschrich, R. Schliebs, Oligomeric beta-amyloid (1–42) induces the expression of Alzheimer disease-relevant proteins in cholinergic SN56.B5.G4 cells as revealed by proteomic analysis, Int. J. Dev. Neurosci. 26 (2008) 301–308.
[14] Y. Hu, J.P Malone, A.M. Fagan, R.R. Townsend, D.M. Holtzman, Comparative proteomic analysis of intra- and interindividual variation in human cerebrospinal fluid, Mol. Cell. Proteomics 4 (2005) 2000–2009.
[15] Z. Xun, R.A. Sowell, T.C. Kaufman, D.E. Clemmer, Quantitative proteomics of a presymptomatic A53T alpha-synuclein *Drosophila* model of Parkinson disease, Mol. Cell. Proteomics 7 (2008) 1191–1203.
[16] M.H. Chin, W.J. Qian, H. Wang, .A. Petyuk, J.S. Bloom, D.M. Sforza, G. Laćan, D. Liu, A.H. Khan, R.M. Cantor, D.J. Bigelow, W.P. Melega, D.G. Camp 2nd, R.D. Smith, D.J. Smith, Mitochondrial dysfunction, oxidative stress, and apoptosis revealed by proteomic and transcriptomic analyses of the striata in two mouse models of Parkinson's disease, J. Proteome Res. 7 (2008) 666–677.
[17] S. Campioni, M.F Mossuto, S. Torrassa, G. Calloni, P.P. de Laureto, A. Relini, A. Fontana, F. Chiti, Conformational properties of the aggregation precursor state of HypF-N, J. Mol. Biol. 379 (2008) 554–567.
[18] J.L. Mazzola, M.A. Sirover, Alteration of intracellular structure and function of glyceraldehyde-3-phosphate dehydrogenase: a common phenotype of neurodegenerative disorders? Neurotoxicology. 23 (2002) 603–609.
[19] S. Carujo, J.M. Estanyol, A. Ejarque, N. Agell, O. Bachs, M.J. Pujol, Glyceraldehyde 3-phosphate dehydrogenase is a SET-binding protein and regulates cyclin B-cdk1 activity, Oncogene 25 (2006) 4033–4042.
[20] T. Müller, C.G. Concannon, M.W. Ward, C.M. Walsh, A.L. Tirniceriu, F. Tribl, D. Kögel, J.H. Prehn, R. Egensperger, Modulation of gene expression and cytoskeletal dynamics by the amyloid precursor protein intracellular domain (AICD), Mol. Biol. Cell. 18 (2007) 201–210.
[21] D. Wessel, A. Flügge, Method for the quantitative recovery of protein in dilute solution in the presence of detergents and lipids, Anal. Biochem. 138 (1984) 141–143.
[22] D.F. Hochstrasser, A. Patchornik, C.R. Merril, Development of polyacrylamide gels that improve the separation of proteins and their detection by silver staining, Anal. Biochem. 173 (1998) 412–423.
[23] V. Neuhoff, N. Arold, D. Taube, W. Ehrhardt, Improved staining of proteins in polyacrylamide gels including isoelectric focusing gels with clear background at nanogram sensitivity using Coomassie Brilliant Blue G-250 and R-250, Electrophoresis 9 (1988) 255–262.
[24] H.R. Saibil, Chaperone machines in action, Curr. Opin. Struct. Biol. 18 (2008) 35–42.
[25] R. Arya, M. Mallik, S.C. Lakhotia, Heat shock genes — integrating cell survival and death, J. Biosci. 32 (2007) 595–610.
[26] M.D. Schaller, C.A. Borgman, B.S. Cobb, R.R. Vines, A.B. Reynolds, J.T. Parsons, pp125FAK a structurally distinctive protein–tyrosine kinase associated with focal adhesions, Proc. Natl. Acad. Sci. U. S. A. 89 (1992) 5192–5196.
[27] M.D. Schaller, Biochemical signals and biological responses elicited by the focal adhesion kinase, Biochim. Biophys. Acta 1540 (2001) 1–21.

[28] I. Karakesisoglou, Y. Yang, E. Fuchs, An epidermal plakin that integrates actin and microtubule networks at cellular junctions, J. Cell Biol. 149 (2000) 195–208.
[29] H.J. Chen, C.M. Lin, C.S. Lin, R. Perez-Olle, C.L. Leung, R.K. Liem, The role of microtubule actin cross-linking factor 1 (MACF1) in the Wnt signaling pathway, Genes Dev. 20 (2006) 1933–1945.
[30] M.A. Lovell, S. Xiong, W.R. Markesbery, B.C. Lynn, Quantitative proteomic analysis of mitochondria from primary neuron cultures treated with amyloid beta peptide, Neurochem. Res. 30 (2005) 113–122.
[31] S.J. Shin, S.E. Lee, J.H. Boo, M. Kim, Y.D. Yoon, S.I. Kim, I. Mook-Jung, Profiling proteins related to amyloid deposited brain of Tg2576 mice, Proteomics 4 (2004) 3359–3368.
[32] D.C. David, L.M. Ittner, P. Gehrig, D. Nergenau, C. Shepherd, G. Halliday, J. Götz, Beta-amyloid treatment of two complementary P301L tau-expressing Alzheimer's disease models reveals similar deregulated cellular processes, Proteomics 6 (2006) 6566–6577.
[33] J. Petrak, R. Ivanek, O. Toman, R. Cmejla, J. Cmejlova, D. Vyoral, J. Zivny, C.D. Vulpe, Déjà vu in proteomics. A hit parade of repeatedly identified differentially expressed proteins, Proteomics 8 (2008) 1744–1749.
[34] J.C. Ghosh, T. Dohi, B.H. Kang, D.C. Altieri, Hsp60 regulation of tumor cell apoptosis, J. Biol. Chem. 283 (2008) 5188–5194.
[35] S.R. Kirchhoff, S. Gupta, A.A. Knowlton, Cytosolic heat shock protein 60, apoptosis, and myocardial injury, Circulation 105 (2002) 2899–2904.
[36] S. Xanthoudakis, S. Roy, D. Rasper, T. Hennessey, Y. Aubin, R. Cassady, P. Tawa, R. Ruel, A. Rosen, D.W. Nicholson, Hsp60 accelerates the maturation of pro-caspase-3 by upstream activator proteases during apoptosis, EMBO J. 18 (1999) 2049–2056.
[37] A. Samali, J. Cai, B. Zhivotovsky, D.P. Jones, S. Orrenius, Presence of a pre-apoptotic complex of pro-caspase-3, Hsp60 and Hsp10 in the mitochondrial fraction of Jurkat cells, EMBO J. 18 (1999) 2040–2048.
[38] D. Chandra, G. Choy, D.G. Tang, Cytosolic accumulation of HSP60 during apoptosis with or without apparent mitochondrial release: evidence that its pro-apoptotic or pro-survival functions involve differential interactions with caspase-3, J. Biol. Chem. 282 (2007) 31289–31301.
[39] V. Veereshwarayya, P. Kumar, K.M. Rosen, R. Mestril, H.W. Querfurth, Differential effects of mitochondrial heat shock protein 60 and related molecular chaperones to prevent intracellular beta-amyloid-induced inhibition of complex IV and limit apoptosis, J. Biol. Chem. 281 (2006) 29468–29478.
[40] E.J. Tisdale, Glyceraldehyde-3-phosphate dehydrogenase is required for vesicular transport in the early secretory pathway, J. Biol. Chem. 275 (2001) 2480–2486.
[41] P. Huitorel, D. Pantaloni, Bundling of microtubules by glyceraldehyde-3-phosphate dehydrogenase and its modulation by ATP, Eur. J. Biochem. 150 (1985) 265–269.
[42] R. Singh, M.R. Green, Sequence-specific binding of transfer-RNA by glyceraldehyde-3-phosphate dehydrogenase, Science 259 (1993) 365–368.
[43] G. Morgenegg, G.C. Winkler, U. Hübscher, C.W. Heizmann, J. Mous, C.C Kuenzle, Glyceraldehyde-3-phosphate dehydrogenase is a nonhistone protein and a possible activator of transcription in neurons, J. Neurochem. 47 (1986) 54–62.
[44] M.R. Hara, N. Agrawal, S.F. Kim, M.B. Cascio, M. Fujimuro, Y. Ozeki, M. Takahashi, J.H. Cheah, S.K. Tankou, L.D. Hester, C.D. Ferris, S.D. Hayward, S.H. Snyder, A. Sawa, S-nitrosylated GAPDH initiates apoptotic cell death by nuclear translocation following Siah1 binding, Nat. Cell Biol. 7 (2005) 645–646.
[45] D.M. Chuang, C. Hough, V.V. Senatorov, Glyceraldehyde-3-phosphate dehydrogenase, apoptosis, and neurodegenerative diseases, Annu. Rev. Pharmacol. Toxicol. 45 (2005) 269–290.
[46] Z. Dastoor, J.L. Dreyer, Potential role of nuclear translocation of glyceraldehyde-3-phosphate dehydrogenase in apoptosis and oxidative stress, J. Cell Sci. 114 (2001) 1643–1653.
[47] F. Magherini, C. Tani, T. Gamberi, A. Caselli, L. Bianchi, L. Bini, A. Modesti, Protein expression profiles in *Saccharomyces cerevisiae* during apoptosis induced by H_2O_2, Proteomics 7 (2007) 1434–1445.
[48] M.D. Basson, An intracellular signal pathway that regulates cancer cell adhesion in response to extracellular forces, Cancer Res. 68 (2008) 2–4.
[49] D.H. Crouch, V.J. Fincham, M.C. Frame, Targeted proteolysis of the focal adhesion kinase pp125 FAK during c-MYC-induced apoptosis is suppressed by integrin signalling, Oncogene 12 (1996) 2689–2696.
[50] B. Levkau, B. Herren, H. Koyama, R. Ross, E.W. Raines, Caspase-mediated cleavage of focal adhesion kinase pp125FAK and disassembly of focal adhesions in human endothelial cell apoptosis, J. Exp. Med. 187 (1998) 579–586.
[51] J. Grossmann, M. Artinger, A.W. Grasso, H.J. Kung, J. Scholmerich, C. Fiocchi, A.D. Levine, Hierarchical cleavage of focal adhesion kinase by caspases alters signal transduction during apoptosis of intestinal epithelial cells, Gastroenterology 120 (2001) 79–88.
[52] M.F. Mian, C. Kang, S. Lee, J.H. Choi, S.S. Bae, S.H. Kim, Y.H. Kim, S.H. Ryu, P.G. Suh, J.S. Kim, E. Kim, Cleavage of focal adhesion kinase is an early marker and modulator of oxidative stress-induced apoptosis, Chem. Biol. Interact. 171 (2008) 57–66.
[53] L. Zhang, G.Q. Xing, J.L. Barker, Y. Chang, D. Maric, W. Ma, B.-S. Li, D.R. Rubinow, α-Lipoic acid protects rat cortical neurons against cell death induced by amyloid and hydrogen peroxide through the Akt signalling pathway, Neurosci. Lett. 312 (2001) 125–128.